DOI 10.1007/s11223-022-00363-w
Strength of Materials, Vol. 53, No. 6, November, 2021

INFLUENCE OF YAG CONCENTRATION AND PRESSING TIME ON WEAR OF Si_3N_4 BASED CERAMICS

A. Brusilová,[1] Z. Gábrišová,[2] P. Švec,[3] and A. Schrek[4]

UDC 539.4

Abrasive wear resistance of Si_3N_4 strongly depends on its microstructure, in particular, grain morphology. In this work, the effects of β-content, β-Si_3N_4 grain growth, and mechanical properties on wear resistance of silicon nitride-based ceramics were investigated. Ceramic rollers containing 5, 7, and 10 wt.% of YAG (yttrite aluminum garnet $Y_3Al_5O_{12}$) were produced by the hot-pressing technology. The pressing times of 5, 15, and 30 min were used for various ceramic rollers. The weakest microstructure constituent was the brittle crystal boundary phase that broke and chipped off during the wear test. On the base of wear measurements, where the volume loss was inversely proportional to the hardness of ceramics, the wear resistance of ceramics was described by the model $V \sim HV^{-1}$.

Keywords: silicon nitride, microstructure, hardness, fracture toughness, wear resistance.

Introduction. Si_3N_4-based ceramics is a promising material for friction nodes working at extremely high temperatures in abrasive and corrosive environments. It combines high hardness with good fracture toughness, low cofficient of friction, excellent thermal shock resistance, good chemical stability, low weight, and high wear and corrosion resistance [1–3]. It does not deteriorate at high temperatures, so it is used in automotive engines and gas turbines, including the turbocharger rotor. Its main applications are in exhaust valves for combustion engines, heat exchange, seals, pistons, combustion chambers, and cutting tools. Very high-quality bodies developed for these high-reliability applications are available today and can be used in many heavy-duty mechanical, thermal, and wear conditions [4–6].

The mechanical and tribological properties of a material are closely related to the nature and structure of its constitutive elements. The realization of a material with good properties can be achieved through the control of many factors: phase composition of the starting powders, type and amount of sintering additives, processing parameters (time, temperature, pressure) and microstructure (grain size and morphology) [7–9]. The microstructure is recognized as one of the most important factors in achieving good mechanical and tribological properties. The base assumption to maximal reliability achieving is homogeneous microstructure with such grain size and morphology which is able to provide higher strength and higher parameters of fracture mechanics [10, 11]. Lange [12] was the first to report that the α-Si_3N_4 grain morphology in material was mainly affected by starting powder. Powders with high α-phase content can produce materials with better mechanical properties due to elongated β grains resulting from the α- to β-phase transformation at high temperatures during sintering [13]. Nakamura et al. [14] also investigated the microstructure effect on tribological properties and reported that wear increased with the β-Si_3N_4 phase ratio. The

Faculty of Mechanical Engineering, Slovak University of Technology in Bratislava, Bratislava, Slovakia ([1]lena.brusilova@stuba.sk; [2]zuzana.gabrisova@stuba.sk; [3]pavol.svec@stuba.sk; [4]alexander.schrek@stuba.sk).
Translated from Problemy Prochnosti, No. 6, p. 119, November – December, 2021. Original article submitted January 14, 2020.

grain size is the another factor controlling the tribological properties of ceramics. Zutshi et al. [15] determined the relation of wear and microstructure, whereas the wear volume increased with microstructure coarsening, despite the increase in strength and toughness.

Abrasive wear is the most common mechanism of ceramic material removal. There are two types of mechanisms involved in abrasive wear: microcutting and microcracking [16, 17]. The mechanisms of microcutting can be described by the model derived from Rabinowitz's conception of abrasive wear mechanism [18]. In this model, the abrasive particle of a conic shape makes grooves on the surface of the solid body. The removed material volume V can be described as follows:

$$V = \frac{Fl}{\pi \tan \alpha \, HV}, \tag{1}$$

where F is the force necessary to get the abrasive particle into the abraded material, l is the length of a groove on the surface if the cone moves in parallel with the worn material surface, HV is the hardness of ceramics, and α is the angle of the cone, participating in the surface grooving. It follows from Eq. (1) that the removed material volume depends on a single material property, namely hardness HV.

If we consider the mechanism of microcracking, the abrasive particle creates a crack in the plane of the load axis after the overrun of the specific limit value of the load. Cracks spread to the specimen surface, where they can develop into a fracture [19–21]. The volume of wear V can be expressed as follows:

$$V = \frac{F^{9/8} l}{K_{\mathrm{Ic}}^{1/2} HV} \left(\frac{E}{HV} \right)^{4/5}, \tag{2}$$

where l is the abrasive particle path length, F is the load acting on the abrasive particle, K_{Ic} is fracture toughness of the ceramics, HV is the hardness of the ceramics, and E is the elastic modulus of the worn ceramic material. According to Eq. (2), the removed material volume V is dependent on three material properties: the elastic modulus E, fracture toughness K_{Ic}, and hardness HV.

According to some works [18, 22] the ratio K_{Ic}/HV is the main characteristic determining the dominant wear mechanisms of brittle materials during abrasive wear at the point of contact. The mechanism of microcutting is dominant at high values of this ratio and fracture toughness, i.e., wear volume depends on hardness as ($V \sim HV^{-1}$). The brittle fracture dominates at low values of the K_{Ic}/HV ratio, i.e., wear will increase with decreasing fracture toughness ($V \sim K_{\mathrm{Ic}}/HV$). According to Eq. (1), the intensity of microcutting decreases with the hardness of ceramics, and according to Eq. (2) the intensity of microcracking decreases with fracture toughness of the worn surface. This can lead to a transition from plastic microcutting to brittle microcracking during abrasive wear [23].

1. Materials and Experiments. Sintering additives are required to produce full-density Si_3N_4 ceramics [24, 25]. The ceramic specimens in this study were produced using Y_2O_3 and Al_2O_3 sintering additives in contents required to form the $Y_3Al_5O_{12}$ garnet (YAG). This phase contributed to the sintering ability of the ceramics [7, 26]. specimens with different contents listed in Table 1 were produced with different sintering times (5, 15, and 30 min) using the hot pressing technology.

The initial powder compositions were wet-mixed in alcohol. After drying and sieving, the powder was compacted in steel dies. The final densification was accomplished using hot-pressing techniques in a nitrogen atmosphere with a purity of 99.99% and an overpressure of 75 kPa. All specimens were hot-pressed at a temperature of 1680℃ and a pressure of 34 MPa.

Densities of the hot-pressed ceramics were measured by Archimedes's method. Hardness and fracture toughness were determined by the Vickers indentation method. The wear resistance was evaluated by grinding the specimen via the pin-on-disk method. Test specimens were placed in contact with corundum grinding paper with a graininess of 120 μm. The grinding trajectory was 125 m, and the pressure was 1.5 MPa. The wear resistance was determined based on the volume loss of the specimens relative to the grinding trajectory. The microstructures of the

TABLE 1. Chemical Composition of Ceramic specimens

Ceramic specimen	content (wt.%)		
	Si_3N_4	Y_2O_3	Al_2O_3
SN10 (5% YAG)	bulk	7.75	2.14
SN12 (7% YAG)	bulk	8.78	3.00
SN15 (10% YAG)	bulk	10.34	4.30

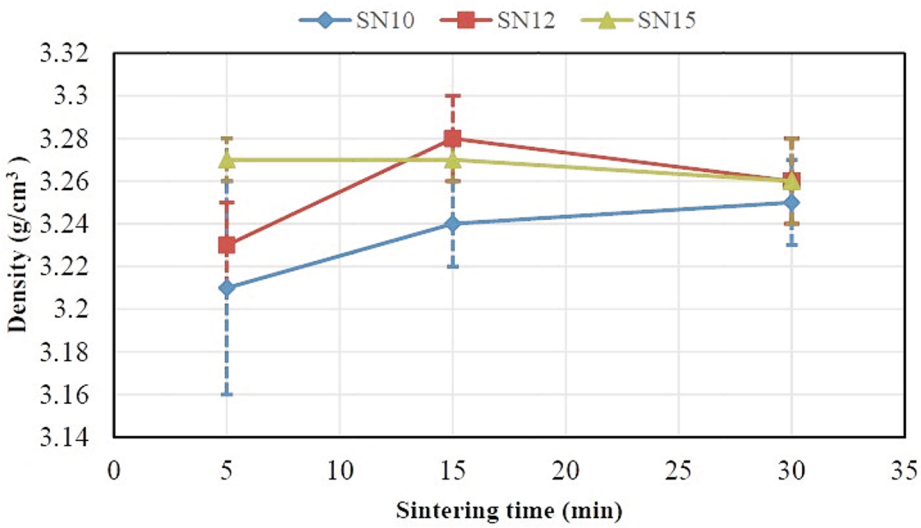

Fig. 1. Effect of pressing time and additive content on density.

hot-pressed ceramics were observed using a scanning electron microscope. To identify the microstructure created, the hot-pressed specimens were subjected to the XRD analysis.

2. Results and Discussion. The effects of density, microstructure, and mechanical properties on the wear resistance of silicon nitride ceramics were evaluated.

2.1. Densification and Microstructure. The starting Si_3N_4 powder contained 96% α-phase composition. The densities of the ceramic specimens were influenced by the amount of additives (Y_2O_3 and Al_2O_3) and the sintering time (Fig. 1). They increased with the content of additives and sintering time from 3.21 to 3.27 g/cm^3. These values corresponded to the relative densities ranging from 97.2 to 98.5%, which indicated a good densification of specimens. The smallest density of 3.21 g/cm^3 was measured in the SN10 specimen with the smallest content of the additives (sintered for 5 min). The highest value of 3.27 g/cm^3 was achieved in the SN12 specimen (sintered for 15 min) and the SN15 specimen (sintered for 5 and 15 min).

Each specimen with different composition and pressing time was analyzed. The phase composition of specimens was identified by the XRD method. Only two phases were found in all specimens, namely α-Si_3N_4 and β-Si_3N_4 phases. Phases with a content below 5% could not be identified using the XRD method. During hot-pressing, the initial α-Si_3N_4 powder was transformed to β-Si_3N_4 phase, which can be seen in Fig. 2. The transformation stage increased with the additive contents and the sintering time. The share of β-Si_3N_4 phase from 42 to 45% was measured by XRD at a shorter sintering time of 5 min for all prepared compositions. There were small differences between separate compositions, but these were within the measurement error of 5%. The 100% transformation of α-Si_3N_4 powder into β-Si_3N_4 phase was achieved only in the SN15 specimens with the highest content of additives (sintered for 30 min).

The study of the microstructure confirmed the effect of the composition on the formed phases. The microstructure consisted of α-Si_3N_4 and β-Si_3N_4 phases. The growing volume of β-Si_3N_4 grains increased with both the additive content and at the sintering time and reached the full β-Si_3N_4 microstructure at the highest additive

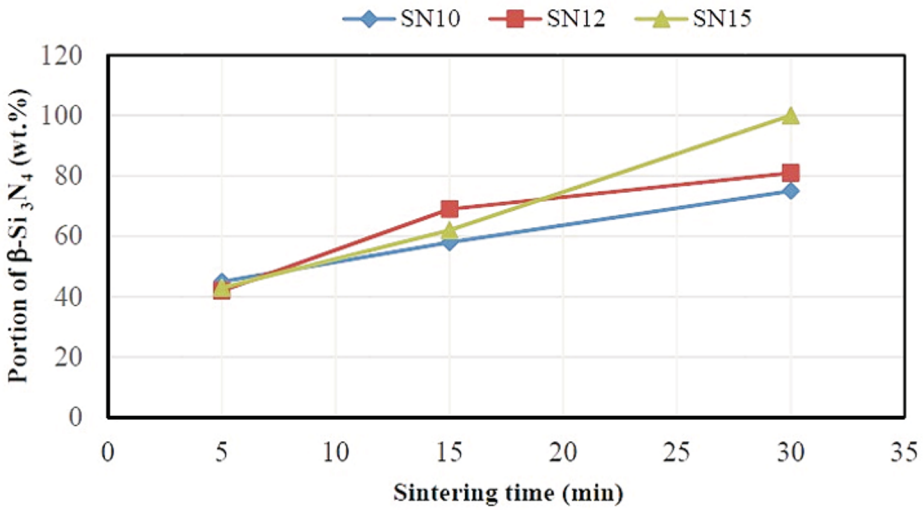

Fig. 2. Effect of pressing time and additive content on share of β-Si_3N_4 phase.

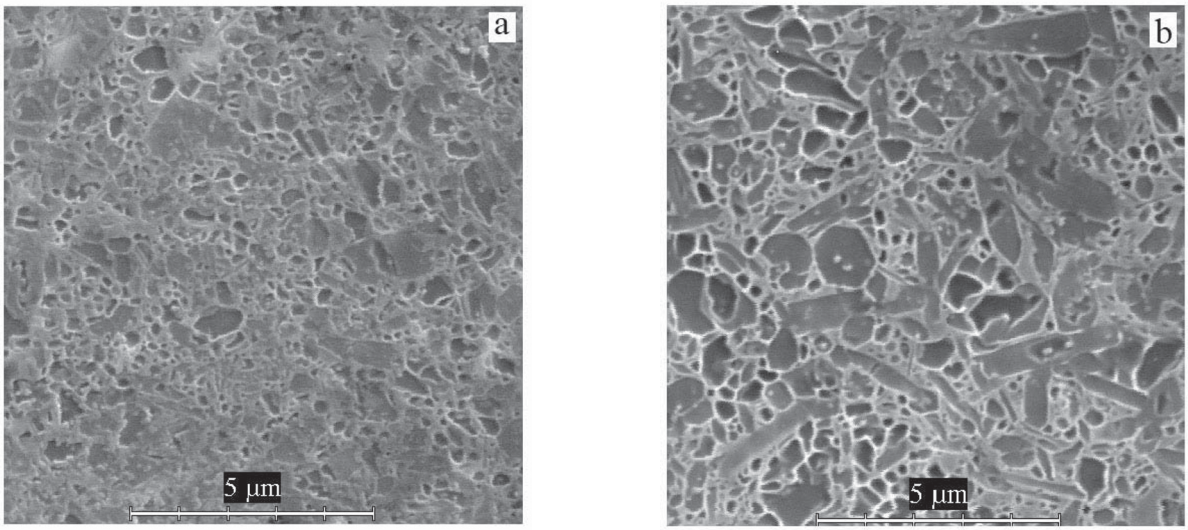

45% β-Si_3N_4 phase ratio (wt.%) 100% β-Si_3N_4 phase ratio (wt.%)

Fig. 3. Grain growth and share increasing of β-Si_3N_4 phase in sample SN15 sintered for 5 (a) and 30 min (b).

content and longest time, which can be seen in Fig. 3 (a specimen SN15 sintered for 30 min). This can be explained by the increase in the transformation velocity at higher additive contents and longer times. With the increase of the additive amount, both the grain size and the ratio of a binding phase at the grain boundary increased. Elimination of residual porosity at the final stage of sintering may be accompanied by excessive grain growth. Grain growth may take place as a result of secondary recrystallization during solid-state sintering.

Excessive grain growth has deleterious effects on the mechanical and tribological properties of ceramic materials. The effect of the additional content and sintering time on the wear of ceramic specimens can be seen in Fig. 4. The volume loss during the wear test dropped with the decreased additions and extended sintering time. The highest wear resistance (the smallest loss) was achieved in the SN15 specimens, and the least wear resistance (the highest loss) was in the SN10 specimens with the smallest addititive's content. The highest wear resistance (the smallest loss) was achieved in specimens with the shortest sintering time of 5 min and the least wear resistance (the highest loss) was observed in specimens with the longest sintering time of 30 min.

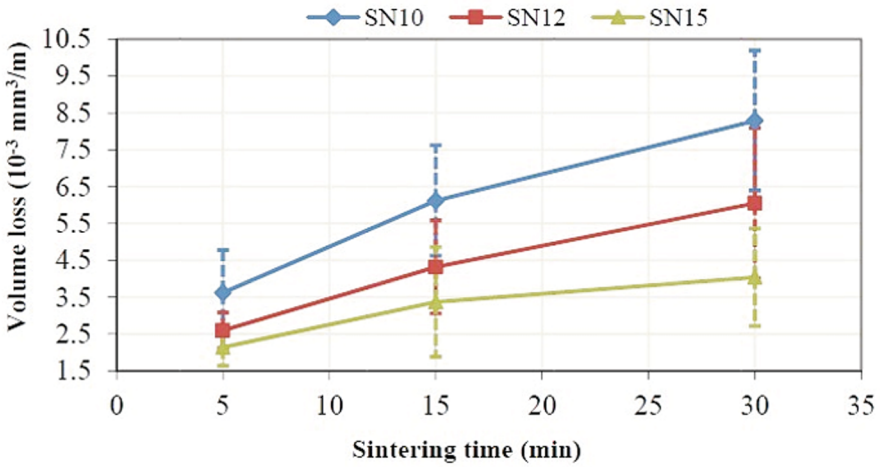

Fig. 4. Effect of pressing time and additive content on wear.

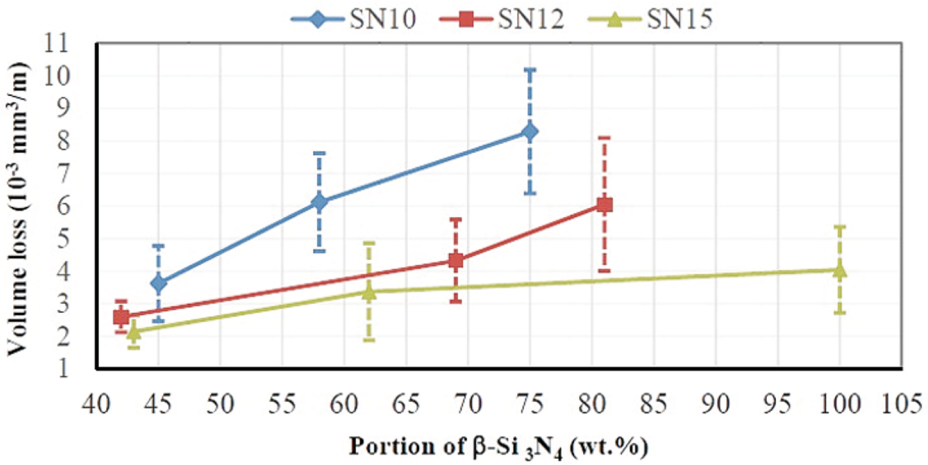

Fig. 5. Effect of β-Si_3N_4 share on wear.

The effect of β-Si_3N_4 share on wear resistance was also observed. According to single curves, the β-Si_3N_4 share had a pronounced effect on wear resistance of ceramics: the volume loss gradually grew with increased β-Si_3N_4 share (Fig. 5). This effect can be caused by coarsed microstructure due to longer sintering time and hardness of equiaxed α-Si_3N_4 grains exceeding that of rod-like β-Si_3N_4 grains [27]. This implies that the wear resistance gradually dropped with increased β-Si_3N_4 share.

2.2. Mechanical Properties and Wear. The effects of the hardness and fracture toughness on the wear properties were studied. The measured values of referred mechanical properties are presented in Figs. 6 and 7. The highest hardness values were achieved for the short pressing time (5 min). After the sintering time extension from 5 to 30 min, the hardness gradually decreased by 0.4–1.0 GPa. The lowest values corresponded to the sintering time of 30 min. This effect was caused by the growth of elongated β-Si_3N_4grains, which hardness was lower than that of equiaxed α-Si_3N_4 grains.

The obtained values showed that the increased fracture toughness (Fig. 7) was related to the growing size of rod-like grains induced by longer pressing times. This was due to the pronounced effect of the aspect ratio of β-Si_3N_4 grains on K_{Ic} values. The microstructure with equiaxed grains achieved lower K_{Ic} values than that containing rod-like grains [27, 28].

The above results indicate that the hardness has a positive effect on wear resistance (Fig. 8), i.e., higher hardness resulted in less wear. As the highest hardness was observed in specimens with the highest content of

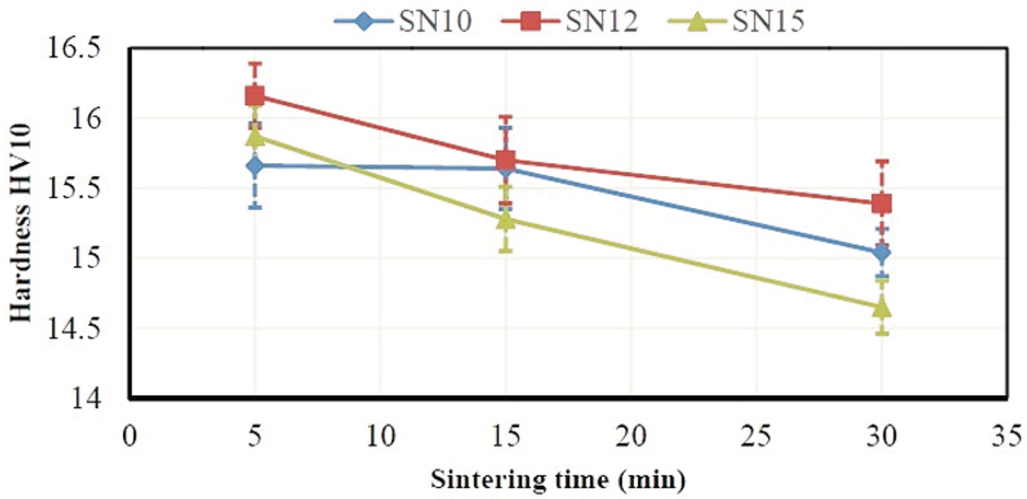

Fig. 6. Effect of pressing time and additive content on hardness.

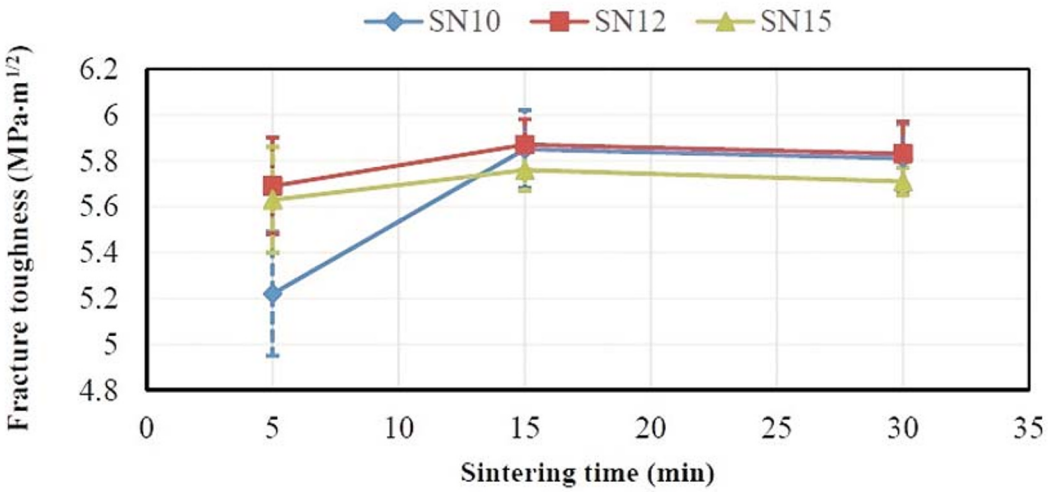

Fig. 7. Effect of pressing time and additive content on fracture toughness.

additives (SN15), these specimens had the smallest volume losses. The highest volume losses were measured in the SN10 specimens with the lowest amount of additives pressed for 5 min. The results in Fig. 8 are in concert with the model ($V \sim HV^{-1}$), where the volume losses V during the wear tests vary inversely in proshare to the hardness HV of the ceramics.

A very interesting development was noted when the effect of fracture toughness on wear was measured (Fig. 9). All compositions showed the same progress. At first, wear increased up to the maximum value. After reaching the maximum value, it decreased slightly. This can be explained by the relationship between the β-Si_3N_4 phase and grain size, but the differences between the separate specimens within each composition were relatively small. The effect of grain size was dominant. The highest grain size was always in the specimen with a middle value of fracture toughness. That means that wear behavior cannot be attributed only to the fracture toughness effect on wear.

Wear behavior may be better described by the model, which reflects the effect of fracture toughness/ hardness ratio on wear rate, as shown in Fig. 10. These relations match very well each separate composition. The higher the value of the calculated ratio, the higher the wear rate. The highest wear rate was observed in SN10 specimens with the smallest content of additives and pressing time of 30 min. The fracture toughness/hardness ratio

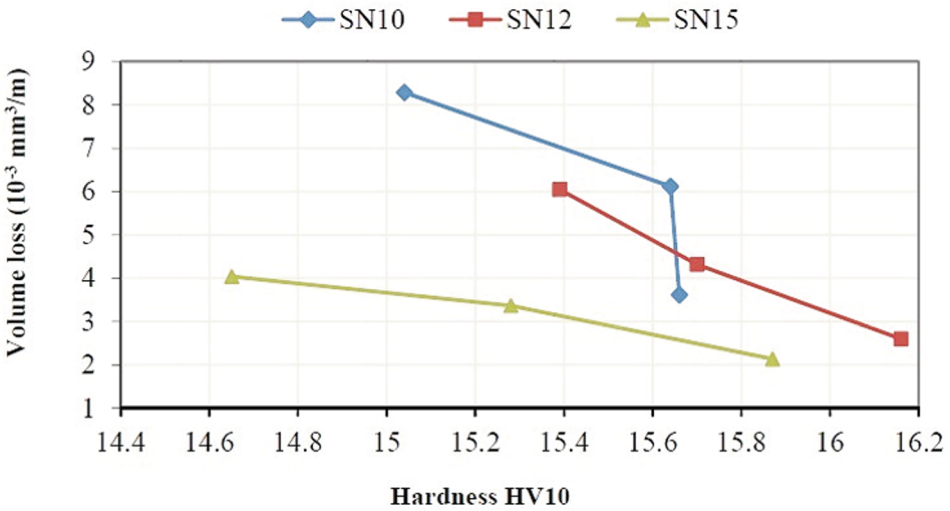

Fig. 8. The hardness effect on the wear of ceramics.

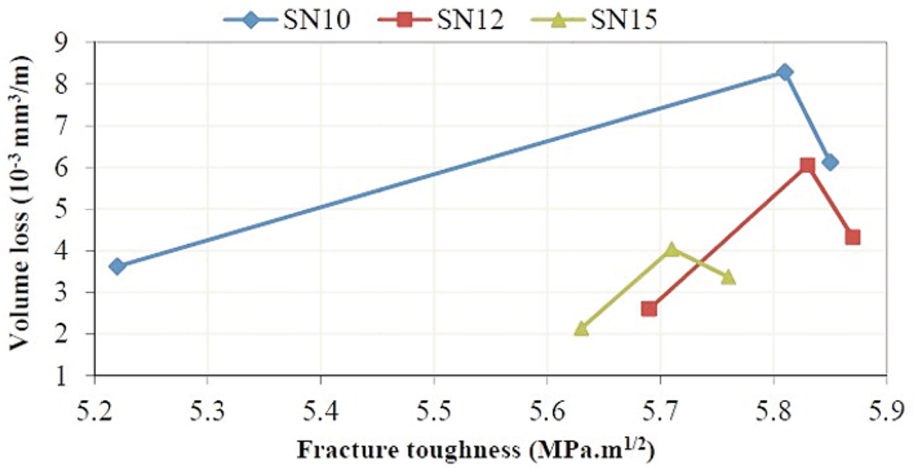

Fig. 9. The fracture toughness effect on the wear of ceramics.

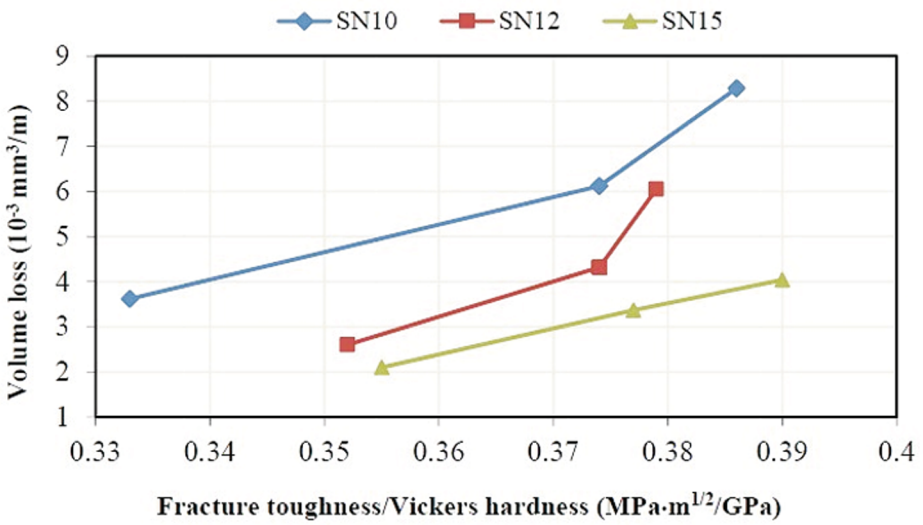

Fig. 10. The fracture toughness/Vickers hardness ratio effect on the wear of ceramics.

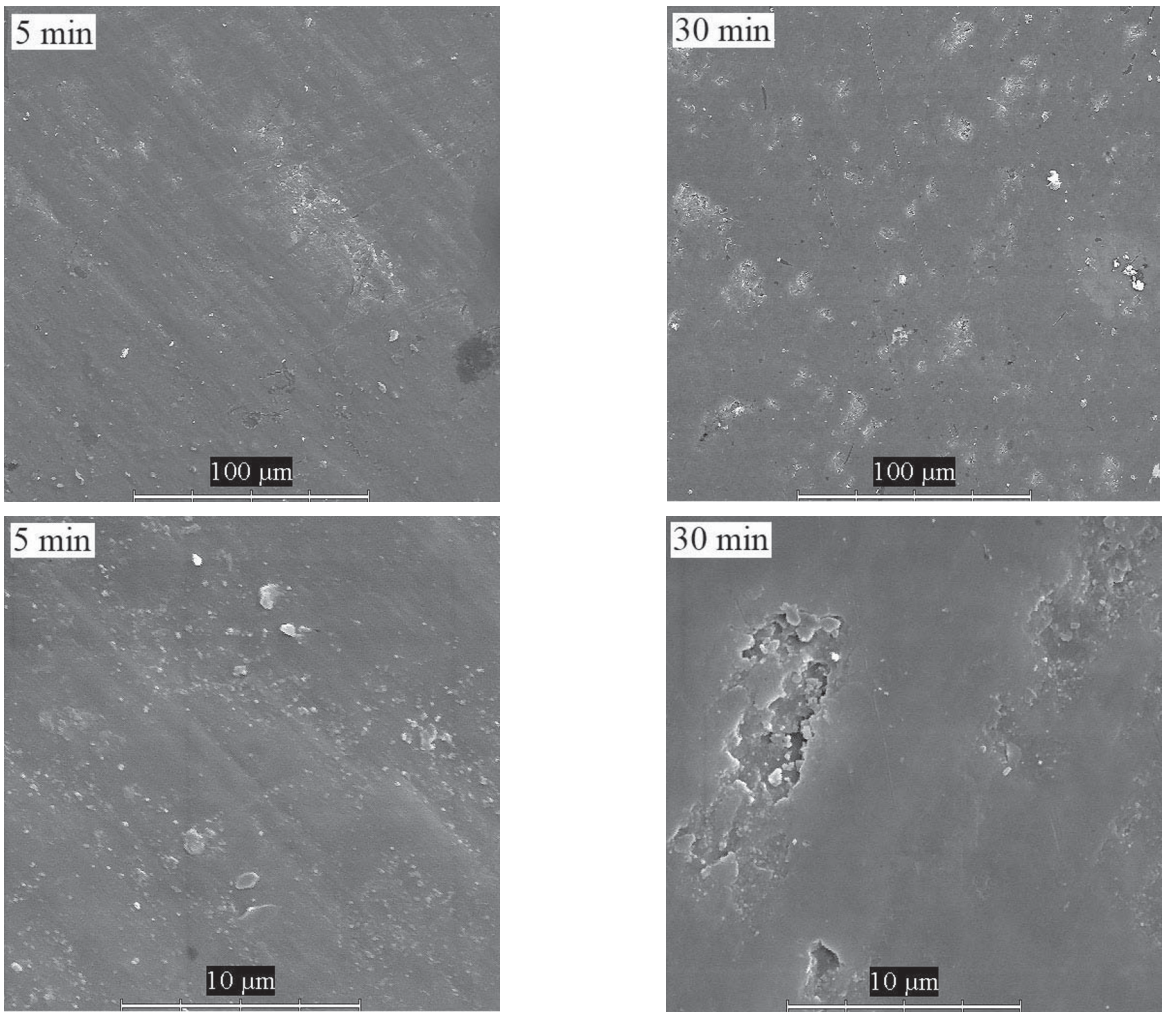

Fig. 11. Surface of SN15ceramic specimens with different pressing times after the wear test.

accurately describes the wear resistance behavior despite the transformation of α-Si_3N_4 phase into the β-Si_3N_4 phase, and the increased wear rate despite the grain growth.

The ceramics surfaces after the wear tests confirmed the earlier described effects of additive content and sintering time on the wear resistance of specimens. The specimens, which were hot-pressed for a longer time, showed greater damage than the specimens pressed for a shorter time (Fig. 11). Much bigger differences among single additive contents were registered with prolongation of sintering time. The specimens with higher contents of additives showed less damage than those with smaller ones (Fig. 12). These specimens have higher shares of the binding phase on the grain boundary. The binding phase has a positive effect on the densification, improving the mechanical properties of ceramic materials. On the other hand, the binding phase is the weakest component of the microstructure [29, 30]. The specimens with higher wear loss showed a greater damage, which was located deeper beneath the surface. The reason was in a brittle crystal boundary phase, which broke and chipped off during the wear tests, as shown in Fig. 11 for the pressing time of 30 min. Prolongation of pressing time resulted in the grain growth, causing lowere wear resistance due to larger volumes were extracted from the surface. The grain growth was caused by stresses induced by different thermal expansion coefficients of crystalline binding phases surrounding single Si_3N_4 grains. The thermal expansion coefficient of binding phase exceeded that of Si_3N_4 (YAG ~ $7 \cdot 10^{-6}$ °C^{-1}, Si_3N_4 ~ $2.2 \cdot 10^{-6}$ °C^{-1}). The K_{Ic} value of this binding phase was nearly twice lower than that of Si_3N_4 [K_{Ic}(YAG) ~ 3 MPa $\cdot$ m$^{1/2}$, K_{Ic}(Si_3N_4) ~ 6 MPa $\cdot$ m$^{1/2}$]. The stresses and low fracture toughness caused easier chipping of grains

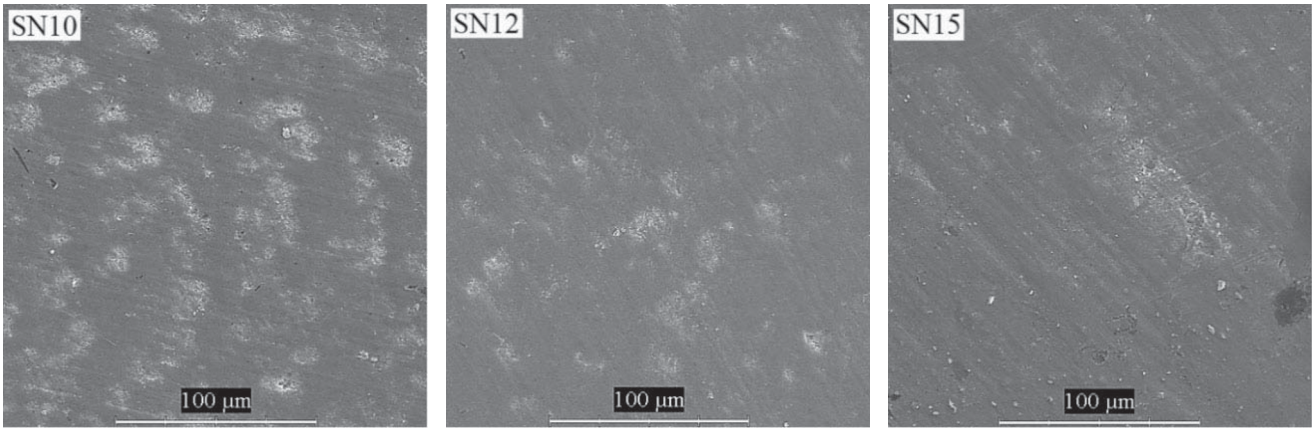

Fig. 12. Surface of ceramic specimens with different content after wear test.

from the surface in the abrasive process. The lower hardness of β-Si_3N_4 rod-like crystals, in comparison to equiaxed α-Si_3N_4 ones, which was growing with the prolongation of pressing time, also influenced this process.

Consistent with the theoretical background, the volume loss depends on hardness ($V \sim HV^{-1}$) when the dominant mechanism of wear is microcutting. If the dominate mechanism is microcracking, the volume loss depends on the hardness/fracture toughness ratio ($V \sim K_{Ic}/HV$). All ceramics surfaces were damaged by microcutting and microcracking. This can be clearly seen from the observed surfaces after the wear tests (Fig. 11). Several scratches and damaged areas are also visible. These areas contain dropped-out material and many microcracks. These characteristic scratches and pits with microcracks were observed in all specimens under study. Thus, both mechanisms caused some wear in all specimens, while the extent of ceramic surface damage increased with pressing time.

Both models could be used to interpret the experimental data on the wear of Si_3N_4 ceramics with corundum abrasive. The experimental data validated the proposed model, which assumed microcutting as the dominant mechanism. Since there were only very small changes in the fracture toughness of separate specimens, the effect of ceramic hardness can be considered as dominant. Thus, the volume loss during wear can be described by the first model ($V \sim HV^{-1}$).

Conclusions. Silicon nitride specimens with various contents of Y_2O_3 and Al_2O_3 sintering additives and various sintering times were fabricated. The effects of these parameters on mechanical properties and wear mechanism were investigated. The effects of hardness and fracture toughness on wear loss were also evaluated. The following conclusions were drawn:

1. The negative effect of grain growth and increased β-Si_3N_4 share on the hardness and wear resistance of silicon nitride-based ceramics was proved. The grain growth increased stresses induced by the difference in thermal expansion coefficients of the crystalline binding phase and single Si_3N_4 grains. The thermal expansion coefficient of the binding phase ($7 \cdot 10^{-6}$ °C^{-1}) exceeded that of Si_3N_4 ($2.2 \cdot 10^{-6}$ °C^{-1}).

2. From the point of view of Si_3N_4 wear resistance in contact with high-hardness abrasives, the weakest microstructure constituent was the brittle crystal boundary phase that broke and chipped off, deteriorating the wear resistance of ceramics. The K_{IC} value of this binding phase (3 MPa $\cdot$ $m^{1/2}$) was twice lower than that of Si_3N_4 (6 MPa $\cdot$ $m^{1/2}$). The stresses and low fracture toughness caused easier grains chipping from the ceramics surface during its wear process.

3. In case of abrasive wear of silicon nitride ceramics conacting with corundum abrasive, the microcutting mechanism, implying the wear resistance dropping with reduced Si_3N_4 hardness, is dominant. This wear mechanism can be accurately described by the proposed model $V \sim HV^{-1}$.

Acknowledgments. The authors are greatful to the Ministry of Education of the Slovak Republic for the financial support of this work under VEGA 1/0298/18 and UVP STU Bratislava ITMS 26240220084.

REFERENCES

1. P. Rutkowski, L. Stobierski, D. Zientara, et al., "The influence of the graphene additive on mechanical properties and wear of hot-pressed Si_3N_4 matrix composites," *J. Eur. Ceram. Soc*., **35**, 87–94 (2015).
2. M. Fellah, M. A. Samad, M. Labaiz, et al., "Sliding friction and wear performance of the nano-bioceramic α-Al_2O_3 prepared by high energy milling," *Tribology Int.*, **91**, 151–159 (2015).
3. Z. T. Ozturk, "Dry sliding wear mechanism of spark plasma sintered Si_3N_4/SiC composites on steel," *Mater. Test*., **56**, 11–12 (2014).
4. S. Hampshire, "Silicon nitride ceramics – review of structure, processing and properties," J. *Achiev. Mater. Manuf. Eng.*, **24**, 43–50 (2007).
5. P. Rutkowski, L. Stobierski, G. Gorny, et al., "Fracture toughness of hot-pressed Si_3N_4-graphene composites," *Mater. Ceram*., **66**, 463–469 (2014).
6. T. Cygan, J. Wozniak, M. Kostecki, et al., "Influence of graphene addition and sintering temperature on physical properties of Si_3N_4 matrix composites," *Int. J. Refract. Met. H.*, **57**, 19–23 (2016).
7. O. Penas, R. Zenati, J. Dubois, and G. Fantozzi, "Processing, microstructure, mechanical properties of Si_3N_4 obtained by slip casting and pressureless sintering," *Ceram. Int*., **27**, 591–596 (2001).
8. B. M. Moshtaghioun, D. Gomez-Garcia, A. Dominguez-Rodriguez, and R. I. Todd, "Grain size dependence of hardness and fracture toughness in pure near fully-dense boron carbide ceramics," *J. Eur. Ceram. Soc.*, **36**, 1829–1834 (2016).
9. Y. Chaochao, J. Yan, Y. Xinyan, et al., "Effect of temperature and pre-sintering on phase transformation, texture and mechanical properties of silicon nitride ceramics," *Mater. Sci. Eng. A*, **731**, 140–148 (2018).
10. G. A. Gogotsi, "Deformation, fracture resistance and heat resistance of elastic and inelastic ceramics," *Strength Mater.*, **45**, No. 2, 248–255 (2013), https://doi.org/10.1007/s11223-013-9454-1.
11. J. Hongsheng, L. Jiaqi, N. Rui, et al., "Fabrication of β-Si_3N_4 with high thermal conductivity under ultra-high pressure," *Ceram. Int.*, **44**, 23288–23292 (2018).
12. F. F. Lange, "Powder vehicle hot-pressing technique," *Am. Ceram. Soc. Bull.*, **52**, 563–565 (1973).
13. S. H. Rhee, J. D. Lee, and D. Y. Kim, "Effect of α-Si_3N_4 initial powder size on the microstructural evolution and phase transformation during sintering of Si_3N_4 ceramics," *J. Eur. Ceram. Soc.*, **20**, 1787–1794 (2000).
14. M. Nakamura, K. Hirao, S. Sakaguchi, et al., in: *25th Annual Conference on Composites, Advanced Ceramics, Materials, and Structures: A: Ceramic Engineering and Science Proceedings*, Volume 22, Issue 3 (2008), pp. 203–208, https://doi.org/10.1002/9780470294680.ch24.
15. A. Zutshi, R. A. Haber, and D. E. Niesz, "Processing, microstructure, and wear behavior of silicon nitride hot-pressed with alumina and yttria," *J. Am. Ceram. Soc*., **77**, 883–890 (1994).
16. H. Soleimani and M. Moavenian, "Tribological aspects of wheel–rail contact: a review of wear mechanisms and effective factors on rolling contact fatigue," *Urban Rail Transit*, **4**, 227–237 (2017).
17. K.-H. Zum Gahr, *Microstructure and Wear of Materials*, Elsevier, Amsterdam; New York (1987).
18. E. Rabinowicz, *Friction and Wear of Materials*, John Wiley and Sons, New York (1995).
19. M. H. Bocanegra-Bernal and B. Matovic, "Dense and near-net shape fabrication of Si_3N_4 ceramics," *Mater. Sci. Eng. A*, **500**, 130–149 (2009).
20. S. M. Hsu and M. Shen, "Wear of ceramics," *Wear*, **256**, 867–878 (2004).
21. W. G. Chang, W. S. Gi, H. B. Woon, et al., "Fabrication of pressureless sintered Si_3N_4 ceramic balls by powder injection molding," *Ceram. Int*., **45**, 6418–6424 (2019).
22. J. A. Williams, "Wear and wear particles – some fundamentals," *Tribology Int*., **38**, 863–870 (2005).
23. E. Medvedovski, "Wear resistant engineering ceramics," *Wear*, **249**, 821–828 (2001).
24. Yu. G. Gogotsi, V. P. Zavada, and V. V. Traskovskii, "Some features of the strength properties of silicon nitride ceramics at high temperature," *Strength Mater*., **19**, No. 11, 1555–1559 (1987), https://doi.org/10.1007/BF01523043.
25. O. A. Lukianova, V. Yu. Novikov, A. A. Parkhomenko, and V. V. Sirota, "Microstructure of spark plasma-sintered silicon nitride ceramics," *Nanoscale Res. Lett.*, **12**, 1–6 (2017).

26. Y. Chaochao, Y. Xinyan, Z. Hui, et al., "In-situ synthesis of YAG and Si_3N_4 powders with enhanced mechanical properties," *J. Alloy. Compd.*, **731**, 813–821 (2018).
27. M. Nakamura and K. Hirao, "Wear behaviour of α-Si_3N_4 ceramics," *Wear*, **254**, 94–102 (2003).
28. H. Kawaoka, Y. H. Choa, and Y. K. Niihara, "Effect of α/β phase ratio on microstructure and mechanical properties of silicon nitride ceramics," *J. Mater. Res.*, **16**, 2264–2270 (2001).
29. B. T. Lee, B. D. Han, and H. D. Kim, "Comparison of fracture characteristic of silicon nitride ceramics with and without second crystalline phase," *Mater. Lett.*, **58**, 74–79 (2003).
30. H. Emoto and M. Mitomo, "Control and characterization of abnormally grown grains in silicon nitride ceramics," *J. Eur. Ceram. Soc.*, **17**, 797–804 (1997).